

VLBL Study Group-H2B-2  
IHEP-EP-2001-02  
Ames-HET-01-08  
November 1, 2018

# On the Optimum Long Baseline for the Next Generation Neutrino Oscillation Experiments

Yifang Wang

Institute of High Energy Physics, Chinese Academy of Sciences  
Beijing 100039, China

Kerry Whisnant and Bing-Lin Young

Department of Physics and Astronomy, Iowa State University  
Ames, Iowa 50011, U.S.A.

## Abstract

For high energy long baseline neutrino oscillation experiments, we propose a Figure of Merit criterion to compare the statistical quality of experiments at various baseline lengths under the condition of identical detectors and a given neutrino beam. We take into account all possible experimental errors under general consideration. In this way the Figure of Merit is closely related to the usual statistical criterion of number of sigmas. We use a realistic neutrino beam for an entry level neutrino factory and a possible superbeam from a meson source and a 100 kt detector for the calculation. We considered in detail four baseline lengths, 300 km, 700 km, 2100 km and 3000 km, in the neutrino energy range of 0.5-20 GeV for a 20 GeV entry level neutrino factory and a 50 GeV superbeam. We found that the very long baselines of 2100 km and 3000 km are preferred for the neutrino factory according to the figure of merit criterion. Our results also show that, for a neutrino factory, lower primary muon energies such as 20 GeV are preferred rather than higher ones such as 30 or 50 GeV. For the superbeam, the combination of a long baseline such as 300 km and a very long baseline like 2100 km will form a complete measurement of the oscillation parameters besides the CP phase. To measure the CP phase in a superbeam, a larger detector (a factor 3 beyond what is considered in this article) and/or a higher intensity beam will be needed to put some significant constraints on the size of the CP angle.

# 1 Introduction

Neutrino oscillations are to date the only experimental indication of physics beyond the standard model that may further expand the horizon of our most basic knowledge of nature. Although the existing data from Super-Kamiokande experiment [1] and the various other corroborating experiments [2] offer very strong indications of neutrino oscillations, the oscillation parameters have not been determined with sufficient accuracy and an appearance experiment have not been convincingly performed. In the ongoing neutrino oscillation experiments and those of the next generation under construction, some of the parameters will be probed with greater accuracy but others may not yet be accessible. Hence more experiments designed to look for the missing information, to carry out appearance experiments, and to probe the known parameters with even greater accuracy are desirable.

In this article we propose a criterion for the determination in general terms and on a global scale the overall quality of long baseline (LBL) experiments. We focus on high energy neutrino beams in the range of 0.5- 20 GeV with the possibility of  $\tau$  production and CP violation measurement, and distances from 300 km to 3000 km. At the lower end, actually 295 km baseline, is the proposed oscillation experiment [3] using the neutrino beam from the newly approved high intensity 50 GeV proton synchrotron in Japan called HIPA [4] with the Super-Kamiokande detector or its updated version. The 700 km baseline is close to the first group of next generation LBL experiments: MINOS [5], ICARUS [6] and OPERA [7], all having a baseline of about 730 km. The 2100 km distance is a possibility for a very long baseline LBL experiment, called H2B, under discussion [8, 9]. The neutrino beam would be from HIPA and the detector, tentatively called the Beijing Astrophysics and Neutrino Detector (BAND), will be located in Beijing, China. The 3000 km baseline has been discussed extensively in neutrino factory studies [10] although particular accelerator and detector sites have not been formally identified.

To compare different experiments is usually difficult. It requires knowledge of the actual detectors, their different systematics, and their neutrino beams. This is beyond the scope of the present work. So for a possible yet meaningful comparison we assume that all experiments have identical detectors and share a given neutrino beam. We believe that our present idealized approach allows us to make a meaningful comparison of the capabilities of the various baseline experiments in general terms and will be useful for the choice of the most suitable baseline length with a given neutrino beam.

In Sec. 2 we present some of the fundamentals of LBL experiments which include the two types of neutrino beams and their beam fluxes that we will use in our calculations. We also list the neutrino charge current cross sections. In Sec. 3 we propose the figure of merit as a criterion to determine the quality of an experiment. Section 4 discusses the figure of merit of the various measurements in the three-neutrino scheme at four baselines: 300 km, 700 km, 2100 km and 3000 km. In practice, for the appearance measurement a superbeam will measure  $\nu_\mu \rightarrow \nu_e, \nu_\tau$  or  $\bar{\nu}_\mu \rightarrow \bar{\nu}_e, \bar{\nu}_\tau$  while a neutrino factory can also measure  $\nu_e \rightarrow \nu_\mu, \nu_\tau$  or  $\bar{\nu}_e \rightarrow \bar{\nu}_\mu, \bar{\nu}_\tau$ . In order to compare the neutrino factory and the neutrino superbeam, in this paper we only use the  $\nu_\mu$  and  $\bar{\nu}_\mu$  beams in our consideration. The measurements considered include  $\nu_e$  and  $\nu_\tau$  appearance, the matter effect, leading oscillation parameters, sign of the leading neutrino mass-square difference, and the CP violation effect. Section 5 contains a brief summary and some pertinent comments, in particular, the comparison of neutrino factories of different primary muon energies.

## 2 Fundamentals of LBL experiments

Due to the extremely weak interaction cross section of neutrinos and beam divergence at a long distance from the source, both the neutrino beam intensity and the detector mass must be maximized in order to have the desired statistics. New technologies for both accelerators and detectors may be required. In the following we discuss briefly some of the fundamentals of the LBL experiment which will be used in our calculations.

### 2.1 Neutrino beams

**Neutrino factory:** The neutrino factory delivers a neutrino beam which contains comparable amount of  $\nu_\mu$  ( $\bar{\nu}_\mu$ ) and  $\bar{\nu}_e$  ( $\nu_e$ ) obtained from the  $\mu^-$  ( $\mu^+$ ) decay in a  $\mu$ -storage ring.

$$\mu^-(\mu^+) \rightarrow \nu_\mu(\bar{\nu}_\mu) + \bar{\nu}_e(\nu_e) + e^-(e^+) \quad (1)$$

The presence of both muon and electron neutrinos is not a problem because they have opposite sign charged leptons in charge current reactions and therefore will not be a background to each other if the detector can distinguish between positive and negative electric charges. A description of the neutrino factory can be found in [11].

The neutrino flux at baseline  $L$  from a neutrino factory of unpolarized muon of energy  $E_\mu$  is given by

$$\frac{d\Phi}{dE_\nu} = \begin{cases} 2x_f^2(3-2x_f)\frac{n_0\gamma^2}{\pi L^2 E_\mu} & \text{for } \nu_\mu \\ 12x_f^2(1-x_f)\frac{n_0\gamma^2}{\pi L^2 E_\mu} & \text{for } \nu_e \end{cases} \quad (2)$$

where  $x_f = E_\nu/E_\mu$ ,  $n_0$  is the number of useful decaying muons, and  $\gamma = E_\mu/m_\mu$  with  $E_\mu$  and  $m_\mu$  being respectively the energy and mass of the muon. Two scenarios of the number of neutrinos in a beam have been considered:  $n_0 = 6 \times 10^{19}/\text{year}$  for an entry level factory and  $n_0 = 6 \times 10^{20}/\text{year}$  for a high performance factory. For a discussion of the neutrino beam spread in a neutrino factor together with some sample plots, see Ref. [12].

**Meson-neutrino superbeam:** Neutrinos from a meson source are obtained from decays of pions and kaons produced by collisions of the primary proton with the nuclear target. The secondary meson beam produced by the collision is sign selected and then focused by a magnetic field. The meson beam is then transported to a vacuum decay pipe, whose length depends on the desired energy of the neutrino. The primary neutrino or anti-neutrino beam consists mostly of the muon flavor from  $\pi^\pm$  and  $K^\pm$  decays in the decay pipe but some impurities of electron neutrinos are expected due to a finite branching ratio of  $\pi^\pm$ ,  $K^\pm$  and  $\mu^\pm$  decaying into electron neutrinos. For example, the NuMI muon neutrino beam at Fermilab contains 0.6% electron neutrinos. The neutrino beam energy profile is more complicated. In general, it can be a wide-band beam covering a broad range of energies, or narrow band beam with a selected, well-defined narrow range of energy.

The neutrino flux at the detector site is determined by the baseline  $L$ , the number of primary protons on target (POT), the proton energy  $E_p$ , and the neutrino energy  $E_\nu$ . The following empirical formula [13] describes the meson production from a proton beam on a nuclear target:

$$\begin{aligned} x_M \frac{d\sigma}{dx_M} &= 2\pi \int x_M E_p \frac{d^3\sigma}{dp^3} P_t dP_t \\ &= 2\pi \int B(1-x_M)^A \frac{1+5e^{-Dx_M}}{(1+P_t^2/C)^4} P_t dP_t \\ &= N_M(1-x_M)^A (1+5e^{-Dx_M}) \end{aligned} \quad (3)$$

where  $N_M$  is a normalization factor,  $p$  the proton 3-momentum,  $x_M$  the Feynman x-variable defined as the momentum of the secondary meson divided by the momentum of proton. A, B, C, and D are numerical parameters which are different for different secondary particles. Table 1. gives their fitted values for  $\pi^+$ ,  $\pi^-$ ,  $K^+$ , and  $K^-$ , taken from Ref.[13]. By taking the general property of Eq. (2), i.e., the  $E^2/L^2$  behavior, to account for the transverse momentum spread due to pion decays, the envelope of the neutrino flux which is the maximum flux at each energy, can be written as,

$$\Phi(E_\nu, L) \propto \frac{E_\nu(1 - x_\nu)^A(1 + 5e^{-x_\nu D})}{L^2} \quad (4)$$

where we take  $x_M \simeq x_\nu \equiv 2E_\nu/E_p$ . The wide or narrow band beam can then be selected from this envelope of the total beam. It is interesting to note that the simple formula given in Eq. (4) can account for the beam design of MINOS at various energies as discussed in Ref. [10]. We should remark that there is a more complete treatment [14] for the energy spectrum of the meson-neutrino beam. However the difference with the above expression for  $E_\nu > 1$  GeV is very small. Owing to its simpler form, we use the above expression in the following calculations.

|         | A      | B         | C       | D      |
|---------|--------|-----------|---------|--------|
| $\pi^+$ | 2.4769 | 5.6817E-2 | 0.57840 | 3.0894 |
| $\pi^-$ | 3.5648 | 5.0673E-2 | 0.68725 | 5.0359 |
| $K^+$   | 1.7573 | 6.3674E-3 | 0.81771 | 5.6915 |
| $K^-$   | 5.4924 | 4.1712E-3 | 0.89038 | 2.2524 |

Table 1: Numerical parameters for meson-neutrino energy spectrum

As a function of  $E_\nu$  and  $L$  the flux of an entry level neutrino factory is given by

$$\Phi_f(E_\nu, L) = 2x_f^2(3 - 2x_f)\frac{n_0^{(f)}\gamma_\mu^2}{\pi L^2 E_\mu} \times 6 \times 10^{22} \quad (5)$$

per thousand tons (kt) per year and per  $\text{cm}^2$ , where  $n_0^{(f)} = 6 \times 10^{19}/\text{year}$ . We will take the primary muon energy to be  $E_\nu = 20$  GeV.

For the neutrino beam of the meson source we take the flux as

$$\Phi_m(E_\nu, L) = (1 - x_\nu)^A(1 + 5e^{-Dx_\nu})\frac{E}{L^2}n_0^{(m)} \times 6 \times 10^{22}. \quad (6)$$

The normalization factor  $n_0^{(m)}$  is determined by the total number of  $\nu_\mu$ 's in the HIPA broad band neutrino beam for  $E_p = 50$  GeV at  $L = 295$  km [3]. This gives  $n_0^{(m)} = 13.7 \times 10^{19}$  in the proper units. We note that Eq. (6) gives only the envelope of the flux, not the actual shape of the energy spectrum. A more precise simulation can be made once the exact beam profile is given.

## 2.2 Interaction cross sections

The detection of the neutrino flavor is through the charge current interaction. For a neutrino energy which is small compared to the mass of the W-boson, the charge current cross sections

for the electron and muon neutrino are given by

$$\sigma_{\nu N}^{(e,\mu)} = 0.67 \times 10^{-38} \text{cm}^2 E_\nu (\text{GeV}) \quad (7)$$

$$\sigma_{\bar{\nu} N}^{(e,\mu)} = 0.34 \times 10^{-38} \text{cm}^2 E_\nu (\text{GeV}) \quad (8)$$

For the tau neutrino, the above expression is subject to a threshold suppression. The threshold for the production of the  $\tau$  is  $E_\tau = 3.46$  GeV. The charge current production cross section of the  $\tau$  is usually given numerically as a function of the neutrino energy. We fit the numerical cross sections [15] from the  $\tau$  threshold to 100 GeV and obtained the following expression

$$\sigma_{\nu N}^{(\tau)} / \sigma_{\nu N}^{(\mu)} = \frac{(E_\nu - E_T)^2}{c_0 + c_1 E_\nu + c_2 E_\nu^2} \theta(E_\nu - E_T), \quad (9)$$

where  $c_0 = -84.988$ ,  $c_1 = 18.317$ , and  $c_2 = 1.194$ . As shown in Fig. 1, the fit, which is valid for  $E_\nu \geq 4.0$  GeV, is good to within 3%. The difference occurs mostly in the neutrino energy region of 20-40 GeV.

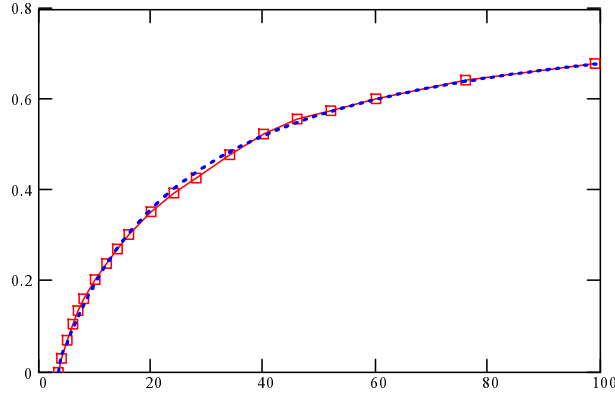


Figure 1: A fit of the numerical ratio of the  $\tau$  to  $\mu$  charge current production cross section from the  $\tau$  threshold to 100 GeV. The boxes are the data points and the dotted curve is the fit. The horizontal axis is the neutrino energy in GeV and the vertical axis is the ratio of  $\tau$  to  $\mu$  production cross sections.

### 3 Statistics and Figure of Merit

Let us consider the oscillation:  $\nu_\alpha \rightarrow \nu_\beta$ . We define two differential number of particle distributions as functions of the neutrino energy and baseline length. In the following we will drop the subscript  $\nu$  and use  $E$  for the neutrino energy :

$$N_{0\alpha}(E, L) = \Phi(E, L) K_t T_y \sigma_\alpha(E) \quad (10)$$

$$N_{0\beta}(E, L) = \Phi(E, L) K_t T_y \sigma_\beta(E) \quad (11)$$

where  $K_t$  is in kilotons and  $T_y$  in years.  $\Phi(E, L)$  is the flux of the  $\nu_\alpha$  and given in Eqs. (5) and (6),  $\sigma_\alpha(E)$  and  $\sigma_\beta(E)$  are the charge current scattering cross sections of  $\nu_\alpha$  and  $\nu_\beta$ . Then

the total number of non-oscillating interacting beam neutrinos at the distance  $L$  over an energy range is given by

$$N_{0\alpha}(L) = \int N_{0\alpha}(E, L) dE, \quad (12)$$

The limits of the energy integration depend on the energy range selected which can be over the whole energy range of the available beam or a selected bin size.

The number of charged leptons of flavor  $\beta$  appearing in the detector, which is the signal for identifying the appearance of  $\nu_\beta$  in the  $\nu_\alpha$  beam, is given by

$$N_{S\beta}(L) = \int P_{\alpha \rightarrow \beta}(E, L) N_{0\beta}(E, L) dE \quad (13)$$

where  $P_{\alpha \rightarrow \beta}(E, L)$  is the oscillation probability for  $\nu_\alpha \rightarrow \nu_\beta$ . Again the integration can be over the whole available energy range of the neutrino beam or a bin size. The averaged oscillation probability over the given energy range is

$$\langle P_{\alpha \rightarrow \beta}(L) \rangle = \frac{N_{S\beta}(L)}{N_{0\beta}(L)} \quad (14)$$

where

$$N_{0\beta}(L) = \int N_{0\beta}(E, L) dE \quad (15)$$

We now define the figure of merit in terms of the physically measurable quantity and its uncertainties:

$$F_M(L) \equiv \frac{\langle P_{\alpha \rightarrow \beta}(L) \rangle}{\delta \langle P_{\alpha \rightarrow \beta}(L) \rangle} \quad (16)$$

where  $\delta \langle P_{\alpha \rightarrow \beta}(L) \rangle$  denotes the uncertainties of  $\langle P_{\alpha \rightarrow \beta}(L) \rangle$ . In the usual definition this is the number of sigma that determines the quality of the measurement. There are in general three sources of uncertainties: (i) the statistical error in the measurement of the charge lepton of flavor  $\beta$  which is as usual  $\sqrt{N_{S\beta}(L) + f_\beta N_{0\beta}}$ , where  $f_\beta N_{0\beta}$  is the number of measured background events, expressed as the fraction  $f_\beta$  of  $N_{0\beta}$ ; (ii) the systematic uncertainty in the calculation of the number of background events from  $N_{0\beta}$ , which can be denoted as  $r_\beta f_\beta N_{0\beta}$ . (iii) the systematic uncertainty in the beam flux and the cross section which we denote as  $g_\beta N_{S\beta}$ . The total error is the quadrature of all these uncertainties. Then the figure of merit can be written as

$$\begin{aligned} F_M(L) &= \frac{N_{S\beta}}{\sqrt{N_{S\beta} + f_\beta N_{0\beta} + (g_\beta N_{S\beta})^2 + (r_\beta f_\beta N_{0\beta})^2}} \\ &= \frac{\langle P_{\alpha \rightarrow \beta}(L) \rangle}{\sqrt{\frac{\langle P_{\alpha \rightarrow \beta}(L) \rangle + f_\beta}{N_{0\beta}(L)} + (g_\beta \langle P_{\alpha \rightarrow \beta}(L) \rangle)^2 + (r_\beta f_\beta)^2}}. \end{aligned} \quad (17)$$

This expression can be generalized to the case when the physical quantity under consideration involves two or more averaged probabilities. In that situation, each probability has its associated uncertainties. In the uncertainty terms we will refer to the linear terms which are inversely proportional to the beam intensity as the statistical terms, and to the quadratic terms as the uncertainty terms.

The value of  $r_\beta$  depends on how well the background is calculated. The value of  $g_\beta$  depends on how well the beam flux and detection cross sections are known. Although  $f_\beta$  is not a physical quantity, it can be estimated from the background of the beam survival measurement. Some of

the error factors for different situations have been estimated in the literature [16, 17, 18, 19, 20]. Many of the early treatments included only statistical errors; we believe that we have included all general uncertainty factors as enumerated above Eq. (17). In Sec. 5 we will compare our results with previous analyses.

The expression of the figure of merit can be simplified if we restrict the energy integration to very narrow bins so that the oscillation probability and the charge current (CC) neutrino cross sections do not vary significantly within the bin, then  $P_{\alpha\rightarrow\beta}(E, L)$  and  $N_{0\beta}(E, L)$  are essentially constant over the range of integration of the neutrino energy. Hence in this narrow bin (NB) approximation we have

$$F_M(L)_j = \frac{P_{\alpha\rightarrow\beta}(E_j, L)}{\sqrt{\frac{P_{\alpha\rightarrow\beta}(E_j, L) + f_\beta}{N_{0\beta}(E_j, L)\Delta E} + (g_\beta P_{\alpha\rightarrow\beta}(E_j, L))^2 + (r_\beta f_\beta)^2}} \quad (18)$$

where  $E_j$  is the central value of the energy of the bin and  $\Delta E$  the bin size, both in GeV. Generally speaking at shorter baselines when the oscillation probability is small and the number of events large, the effect of the background is severe. Typical values of  $f_\beta$  for a water Čerenkov calorimeter are a few per cent [8]. For the value of  $f_\beta$  of water Čerenkov ring imaging detector, see Ref. [3].

We can define the figure of merit over an energy range for a given baseline length  $L$ . It gives the overall statistical significance of the measurement over the energy range. Let the energy range contains  $N_b$  bins. Then, in the narrow bin approximation, the total figure of merit in the energy range is

$$F_M^{(T)}(L) = \sqrt{\sum_{j=1}^{N_b} (F_M(L)_j)^2} \quad (19)$$

The above expressions can be extended to the case of anti-neutrinos, and that containing a mixture of neutrino and anti-neutrino. The quantities associated with the anti-neutrino are defined by replacing the neutrino CC cross section by the corresponding anti-neutrino CC cross section.

## 4 Optimum long baselines

In this section we apply the Figure of Merit to examine the effectiveness of measurements of various relevant quantities at medium and very long baseline oscillation experiments relevant to the next generation LBL experiments. We assume identical detectors at all sites with a neutrino beam reaching to the different sites. To limit the scope of the analysis, we will only discuss the scenario of three neutrinos with MSW-LMA which is the most favorable solution to the solar neutrino problem [21]. The mixing parameters are set as follows:  $\Delta m_{32}^2 \approx \Delta m_{31}^2 = 3.3 \times 10^{-3} eV^2$ ,  $\Delta m_{21}^2 = 5 \times 10^{-5} eV^2$ ,  $\tan^2 \theta_{23} = 1.6$ ,  $\tan^2 \theta_{13} = 0.025$ , and  $\theta_{12} = 45^\circ$ . The leptonic CP phase  $\phi$  is set to be  $90^\circ$ . The earth density has been chosen to be constant of  $\rho = 3 \text{ g/cm}^3$  with equal number of protons and neutrons. Then the matter effect constant  $A/E_\nu$  is  $2.3 \times 10^{-4} eV^2/GeV$ .

As already stated earlier, for the neutrino beam we will take  $E_\mu = 20 \text{ GeV}$  for the neutrino factory and  $E_p = 50 \text{ GeV}$  for the meson beam. For the error parameters, we will use  $r_\beta = 0.1$  and  $g_\beta = 0.05$ , independent of the neutrino flavor and beam type. The value of  $f_\beta$ , taking the value 0.01 and 0.03, may be different for different measurements and neutrino beams and will be given explicitly in the various cases considered below. The beam energy considered ranges from 0.5 to 20 GeV and the bin size is  $\Delta E = 0.5 \text{ GeV}$ . For very long baselines, the cases of

neutrino energy of hundreds of MeV and lower require separate investigations. This is because in such lower energy regime, the solar neutrino energy scale will come into play and the Eqs. (7) and (8) are no longer valid as the quasi-elastic charge interactions [22] become significant. The detector size will be taken to be 100 kt [23] and the running time 3 years. For simplicity we use the narrow bin approximation, Eqs. (18) and (19). We will comment in the Summary and Comments section on neutrino factories of different primary muon energies.

Before we discuss in detail the individual measurements, we summarize the general feature of the contributions of the statistical and uncertainty terms. For the neutrino factory the statistical terms dominate in the lower energy region whose range increases with the baseline length. Away from the dominant region, the statistical and systematic uncertainty terms become comparable with the latter being slightly larger. For the meson neutrino beam, the statistical terms are dominant in regions at both the lower and upper ends of the beam energies. The two types of terms become comparable in the region in between which is sizable. This feature holds even when the beam intensity increases or decreases by an order of magnitude from the sample meson neutrino beam intensity considered below. Hence the statistical terms are critical in the determination of the figure of merit. We can conclude that although the individual figures of merit depend on the details of the beam intensity and the various error factors, the relative figures of merit of different baseline lengths are not too sensitive to the details of the beam profile as long as the correct neutrino beam energy and baseline distance dependence are taken into consideration. Hence the relative figures of merit discussed below should be approximately valid even when the beam intensity profile is not precisely known.

For the total figure of merit as a function of baseline, we only consider the neutrino factory. The use of Eq. (6) for the meson neutrino beam is not meaningful for the total figure of merit in view of the complicated nature of the meson neutrino beam. For comparison we also consider the total figure of merit for neutrino factories of 30 and 50 GeV.

To simplify the numerical calculations, we consider only the case of constant matter density. We use the vacuum oscillation formulae for  $\nu_\mu \rightarrow \nu_\mu$ ,  $\nu_\mu \rightarrow \nu_\tau$ . For  $\nu_\mu \rightarrow \nu_e$  appearance we use the approximate expressions given in Ref. [24]. For the CP phase sensitivity we use the exact formula given in Ref. [25].

#### 4.1 Mixing probability $\sin^2 2\theta_{13}$

The oscillation probability  $P(\nu_\mu \rightarrow \nu_e)$  is a direct measurement of  $\sin^2 2\theta_{13}$  since  $P(\nu_\mu \rightarrow \nu_e) \propto \sin^2 2\theta_{13}$ . The statistical significance of  $P(\nu_\mu \rightarrow \nu_e)$  for a given experiment can be measured by the **figure of merit**. From Eqs. (17) and (18), we have

$$F_M^{(1)}(L) = \frac{\langle P_{\nu_\mu \rightarrow \nu_e}(L) \rangle}{\sqrt{\frac{\langle P_{\nu_\mu \rightarrow \nu_e}(L) \rangle + f_{\nu_e}}{N_{0\nu_e}(L)} + (g_{\nu_\mu} \langle P_{\nu_\mu \rightarrow \nu_e}(L) \rangle)^2 + (r_{\nu_e} f_{\nu_e})^2}} \quad (20)$$

For the error factor  $f_{\nu_e}$ , contributions from the beam are at the level of 0.6% for meson-neutrino beams.<sup>1</sup> We conservatively choose  $f_{\nu_e} = 0.03$  for the conventional meson beam and  $f_{\nu_e} = 0.02$  for the neutrino factory. Now the figure of merit can be readily calculated using Eqs. (20) as functions of the neutrino energy  $E$  at four different baselines: 300 km, 700 km, 2100 km and 3000 km.

To see the importance of the background let us first consider the figure of merit by ignoring the background, i.e., setting  $r = 0$ ,  $g = 0$  and  $f = 0$ . The results are given in Figs. 2(a) and (b). As shown in Fig. 2(a), there is an optimum neutrino energy,  $E_{\text{opt}} = 15$  GeV, independent

---

<sup>1</sup>See Ref. [3] for the water Čerenkov ring imaging detector.



of the baseline, where the figure of merit is at a maximum for the neutrino factory. For the superbeam, each baseline is associated with a different  $E_{\text{opt}}$  and the smaller baseline has higher figure of merit as shown in Fig. 2(b). In these plots and for all those figure of merit plots that follow, the dotted line is for  $L = 3000$  km, the heavy dotted line for  $L = 2100$  km, the dash line for  $L = 700$  km, and the dash-dotted line for  $L = 300$  km. For the very long baseline of 2100 and 3000 km the figures of merit are small and tend to oscillate rapidly at low energies, so we do not show them for  $E < 1.5$  GeV.

We have examined the cases of 30 and 50 GeV neutrino factories and found that their figures of merit as a function of the neutrino energy are similar to those of the 20 GeV case. The  $E_{\text{opt}}$  occurs at roughly the same value and the height of the maximum decreases as the primary muon energy increases.

However, the above picture is changed when the effect of experimental uncertainties are taken into account. As shown in Figs. 2(c) and (d), the figure of merit is generally reduced. For the neutrino factory the figure of merit increases with the baseline length, and for the longer distances like 2100 km is much higher than the shorter distance like 300 km. For the conventional neutrino beams the reduction of the figure of merit at longer distances is less when uncertainties are included, and all distances have comparable figures of merit over the whole energy range. Hence the comparison of Figs. 2(c) and (d) with Figs. 2(a) and (b) demonstrates the importance of the effect of the background in the determination of the relative merits of different baselines. It should be noted that the above results are very sensitive to the value of  $\sin^2 2\theta_{13}$ . For a smaller  $\sin^2 2\theta_{13}$ , the effect of the background is larger and the longer baselines will be better.

Figure (3) gives the total figures of merit, according to Eq. (19), of three neutrino factories as functions of the baseline: 20, 30 and 50 GeV. We extend the baseline to  $10^4$  km to show the variation the total figure of merit. At shorter distance the total figures of merit are roughly the same for all three neutrino factories. Their values are small but increase as the baseline increases. The factory of lower energy will reach a maximum sooner as the baseline increases.

## 4.2 CP phase $\phi$

For three flavors there is one measurable phase in the neutrino mixing matrix which will give rise to a CP-violation effect. Although the effect of CP phase in the hadronic sector is small due to the small Jarlskog factor arising from small quark mixing angles, the large or even maximal mixing angles of the neutrinos suggest that it is not impossible to have a large effect of leptonic CP phase. So we will assume the maximal CP phase,  $\phi = \pi/2$ .

The CP phase  $\phi$  can be measured by looking at the difference of the oscillation probability between  $P(\nu_\mu \rightarrow \nu_e)$  and  $P(\bar{\nu}_\mu \rightarrow \bar{\nu}_e)$  or between  $P(\nu_e \rightarrow \nu_\mu)$  and  $P(\bar{\nu}_e \rightarrow \bar{\nu}_\mu)$ . While the former has to have the matter effect removed in order to obtain the CP effect, the later, under the assumption of CPT conservation, allows a direct isolation of the matter from the CP effect, but it can only be done at a neutrino factory in the case of symmetric matter density which is approximately true and identical  $\nu_e$  and  $\bar{\nu}_e$  beam which is generally difficult to arrange.

We define

$$\Delta P(E, L, \phi) = P_{\nu_\mu \rightarrow \nu_e}(E, L, \phi) - P_{\bar{\nu}_\mu \rightarrow \bar{\nu}_e}(E, L, \phi) \quad (21)$$

The CP phase can be obtained by subtracting the matter effect  $\Delta P(E, L, \phi) - \Delta P(E, L, 0)$ . Then the figure of merit for the leptonic CP phase measurement can be written as

$$F_M^{(2)}(\phi) = \frac{\langle \Delta P(\phi) \rangle - \langle \Delta P(0) \rangle}{N^{(2)}(\phi)}$$

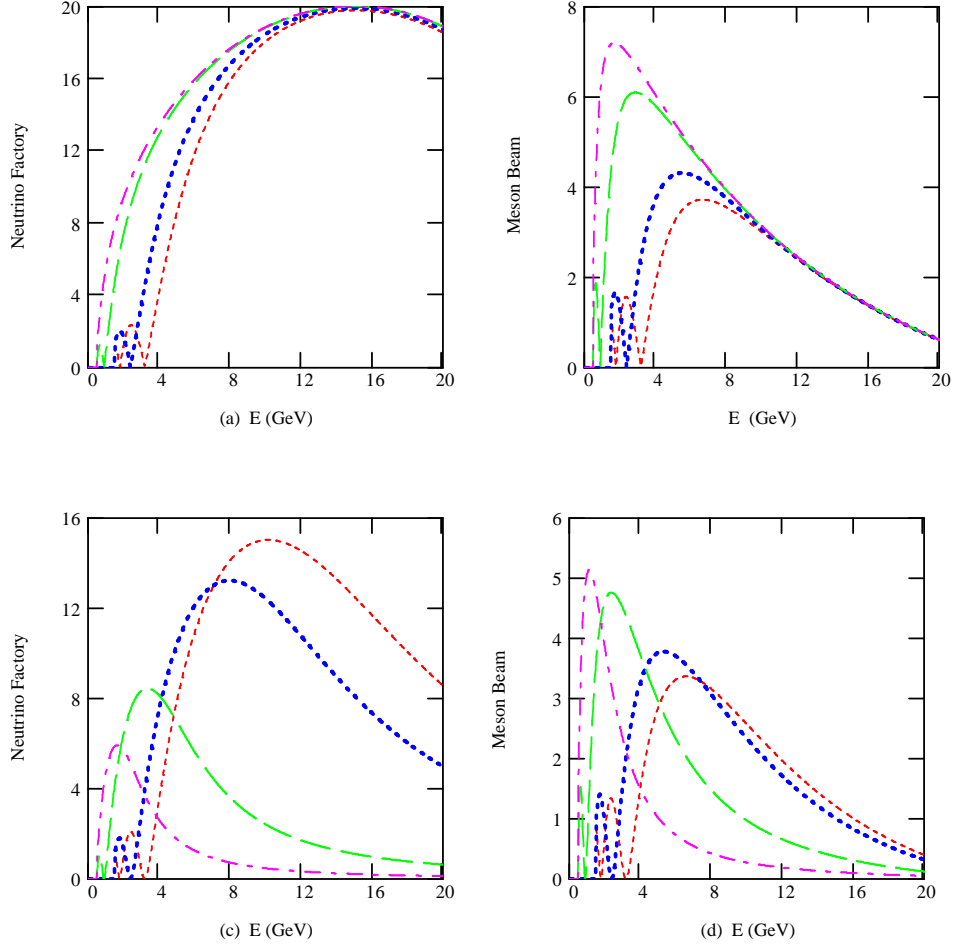


Figure 2: Figure of merit for the  $\sin^2 2\theta_{13}$  measurement at a) neutrino factories without backgrounds, b) meson-neutrino beams without backgrounds, c) neutrino factories with  $f=0.02$  and  $r=0.1$ , and d) meson-neutrino beams with  $f=0.03$  and  $r=0.1$ . In these figures and those that follow the dotted line is for  $L=3000$  km, the heavy dotted line for  $L=2100$  km, the dash line for  $L=700$  km, and the dash-dotted line for  $L=300$  km. The 2000 and 3000 km curves are not shown below 1.5 GeV. The vertical axis is the figure of merit given by Eq. (20) and the horizontal axis is the neutrino energy.

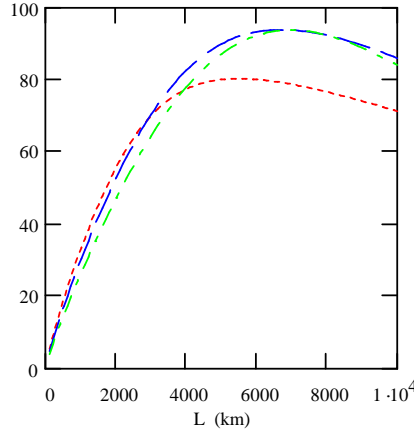


Figure 3: The total figure of merit for  $\sin^2 2\theta_{13}$  as a function of baseline length for neutrino factories of 20 GeV (dot), 30 GeV (dash), and 50 GeV (dashdot). The horizontal axis is the baseline length and the vertical axis is the total figure of merit.

$$N^{(2)}(\phi) = \left( \frac{\langle P(\phi) \rangle + f_{\nu_e}}{N_{0\nu_e}(\phi)} + (r_{\nu_e} f_{\nu_e})^2 + (r_{\bar{\nu}_e} f_{\bar{\nu}_e})^2 \right. \\ \left. + \frac{\langle \bar{P}(\phi) \rangle + f_{\bar{\nu}_e}}{N_{0\bar{\nu}_e}(\phi)} + g^2(\langle P(\phi) \rangle^2 + \langle \bar{P}(\phi) \rangle^2) \right)^{1/2}, \quad (22)$$

where to simplify the notation we have defined all the quantities by retaining the reference to the CP phase and dropping the other variables.

The figures of merit are calculated according to Eq. (22) with  $f = 0.02$  for the neutrino factory and  $f = 0.03$  for the conventional beam. Figure 4(a) shows the figure of merit for neutrino factories with the full uncertainties for the neutrino factory. For  $L/E$  fixed at the optimum energy, the sensitivity to the CP phase  $\phi$  is a factor of 2 better at  $L=2100$  km than that at  $L=300$  km for the neutrino factory. The sensitivity to the CP phase for the conventional neutrino beam is shown in Fig. 4(b). A similar optimum energy also exists and the sensitivity at  $L=2100$  km is about 20% lower than that at  $L=300$  km at their respective peak values. At neutrino factories, the figure of merit over the whole energy range, i.e., the total figure of merit, is much larger for 2100 km than for 300 km as shown in Fig. 5.

### 4.3 Sign of $\Delta m_{32}^2$

Since the vacuum oscillation probability is an even function of  $\Delta m_{kj}^2$ , the presence of the matter effect is necessary in order to measure the sign of  $\Delta m_{32}^2$ . The simplest way is to compare the measured probability  $P_{\nu_\mu \rightarrow \nu_e}$  with the expected values of  $P_{\nu_\mu \rightarrow \nu_e}^+$  and  $P_{\nu_\mu \rightarrow \nu_e}^-$ , where  $P^+$  assumes  $\Delta m_{32}^2 > 0$  and  $P^-$  for  $\Delta m_{32}^2 < 0$ . The channel  $\bar{\nu}_\mu \rightarrow \bar{\nu}_e$  may be more advantageous to use if  $\Delta m_{32}^2 < 0$ . This measurement can only be done if  $\sin^2 2\theta_{13}$  is sizable and the  $\nu_e$  or  $\bar{\nu}_e$  appearance signal is statistically significant. Other channels, such as the  $\nu_\mu \rightarrow \nu_\mu$  survival channel, are less sensitive due to the very small matter dependence. It has been suggested in Ref. [26] that the muons from all channels at the neutrino factory, e.g. the  $\nu_e(\bar{\nu}_e) \rightarrow \nu_\mu(\bar{\nu}_\mu)$  appearance and  $\nu_\mu(\bar{\nu}_\mu) \rightarrow \nu_\mu(\bar{\nu}_\mu)$  survival channels, be included in a given analysis to reduce systematic errors. Here we confine ourselves only to a relatively simple approach to compare

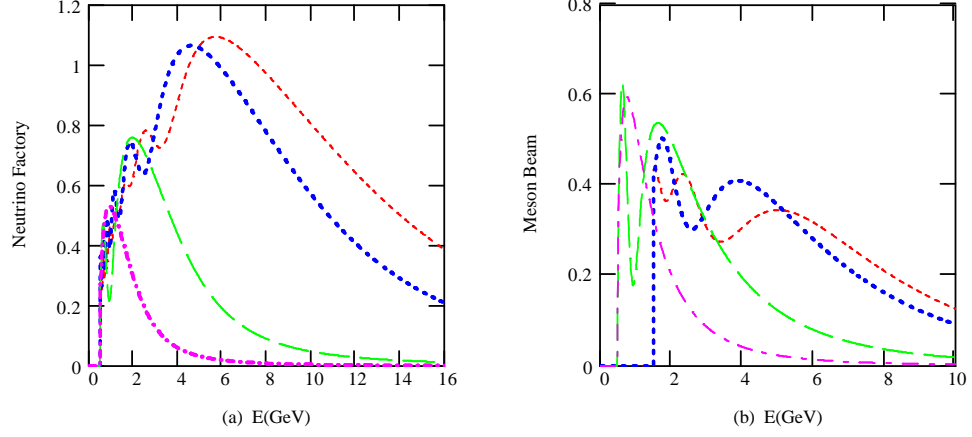


Figure 4: Figure of merit for CP phase measurement at a) neutrino factories with  $f=0.02$  and  $r=0.1$ , and b) meson-neutrino beams with  $f=0.03$  and  $r=0.1$ . The vertical axis is the figure of merit given by Eq. (22) and the horizontal axis is the neutrino energy.

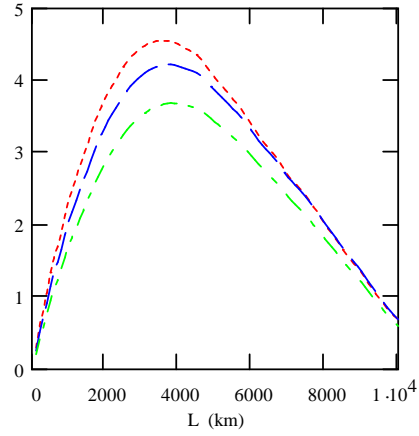


Figure 5: Total figure of merit for CP phase measurement for the neutrino factories of 20 GeV (dot), 30 GeV (dash), and 50 GeV (dashdot). The horizontal axis is the baseline length and the vertical axis is the total figure of merit.

the relative statistical importance at different baselines. The figure of merit in the present case can be written as

$$F_M^{(3)}(L) = \frac{\langle P_{\nu_\mu \rightarrow \nu_e}^+(L) \rangle - \langle P_{\nu_\mu \rightarrow \nu_e}^-(L) \rangle}{\sqrt{\frac{\langle P_{\nu_\mu \rightarrow \nu_e}^+(L) \rangle + f_{\nu_e}}{N_{0\nu_e}(L)} + (g_{\nu_\mu} \langle P_{\nu_\mu \rightarrow \nu_e}^+(L) \rangle)^2 + (r_{\nu_e} f_{\nu_e})^2}} \quad (23)$$

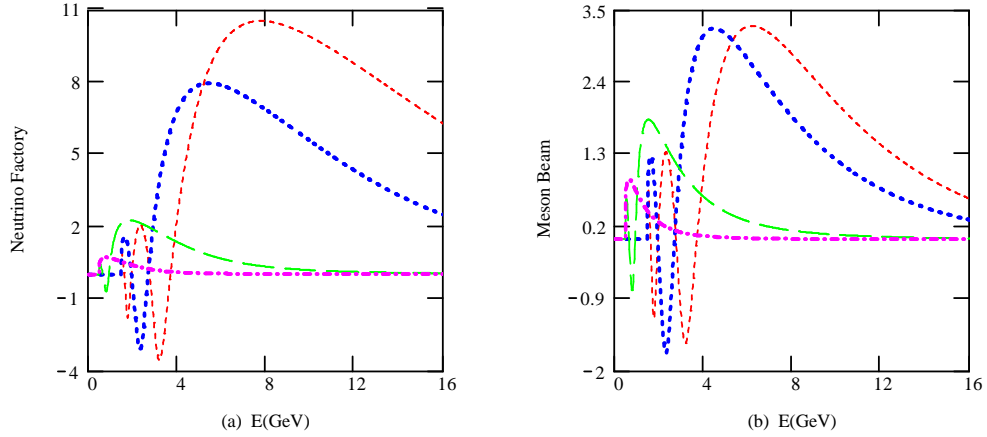


Figure 6: Figure of merit for the sign of  $\Delta m_{32}^2$  at a) neutrino factories with  $f=0.02$  and  $r=0.1$ , and b) meson-neutrino beams with  $f=0.03$  and  $r=0.1$ . The vertical axis is the figure of merit given by Eq. (23) and the horizontal axis is the neutrino energy.

Figure 6 shows the figure of merit as a function of energy at different baselines for neutrino factory and conventional neutrino beams with  $f = 0.02$  for the neutrino factory and  $f = 0.03$  for the conventional neutrino beam. It is clear from the plots that for both beam types, it is much better to have an experiment at longer distance such than at shorter distances. The total figure of merit as a function of the baseline length is give in Fig. 7.

#### 4.4 Matter effect

The matter effect can be measured by looking at the difference between  $\nu_\mu \rightarrow \nu_e$  and  $\bar{\nu}_\mu \rightarrow \bar{\nu}_e$ , although a non-vanishing CP phase,  $\phi \neq 0$ , can alter the result by as much as 20%. The survival channels  $\nu_\mu \rightarrow \nu_\mu$  and  $\bar{\nu}_\mu \rightarrow \bar{\nu}_\mu$  are not very effective for the present purpose since their matter effects appear only in nonleading terms.

The relevant figure of merit is given by

$$F_M^{(4)}(L) = \frac{\langle P_1 \rangle - \langle P_2 \rangle}{\sqrt{\frac{\langle P_1 \rangle + f}{N_{0\nu_e}(L)} + 2r^2 f^2 + \frac{\langle P_2 \rangle + f}{N_{0\bar{\nu}_e}(L)} + g^2(\langle P_1 \rangle^2 + \langle P_2 \rangle^2)}}, \quad (24)$$

where we have dropped the explicit reference to all variables except where it may cause confusion, and denote  $\langle P_1 \rangle \equiv \langle P_{\nu_\mu \rightarrow \nu_e}(L) \rangle$ , and  $\langle P_2 \rangle \equiv \langle P_{\bar{\nu}_\mu \rightarrow \bar{\nu}_e}(L) \rangle$ .

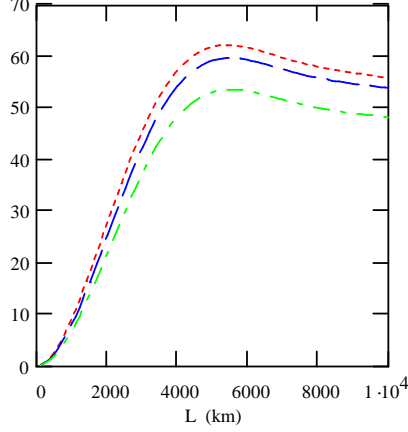


Figure 7: The total figure of merit for the sign of  $\Delta m_{32}^2$  for three neutrino factories of 20 GeV (dot), 30 GeV (dash), and 50 GeV (dashdot). The horizontal axis is the baseline length and the vertical axis is the total figure of merit.

Figure 8 shows the figure of merit as a function of energy at different baselines for a neutrino factory with  $f = 0.02$  and the conventional neutrino beam with  $f = 0.03$ . The plots show clearly that in both cases it is much better to have an experiment at longer baseline than at a shorter one. As show in Fig. 9, the total figures of merit as a function of the baseline length for three neutrino factories, 20, 30 and 50 GeV.

#### 4.5 Precision measurement of $\Delta m_{32}^2$ and $\sin^2 2\theta_{23}$

Although  $\Delta m_{32}^2$  and  $\sin^2 2\theta_{23}$  have been measured at Super-K and hopefully will be further improved by K2K, MINOS, OPERA and ICARUS, it is still interesting to measure them at different baselines and possibly improve the precision.  $\Delta m_{32}^2$  and  $\sin^2 2\theta_{23}$  can be directly related to the survival probability  $P(\nu_\mu \rightarrow \nu_\mu)$ . The figure of merit can be written as

$$F_M^{(5)}(L) = \frac{1 - \langle P \rangle}{\sqrt{\frac{\langle P \rangle + f}{N_{0\nu_\mu}(L)} + r^2 f^2 + (g \langle P \rangle)^2}}, \quad (25)$$

where  $\langle P \rangle \equiv \langle P_{\nu_\mu \rightarrow \nu_\mu}(L) \rangle$ .

Figure 10 shows the figure of merit at different baselines for neutrino factories and conventional neutrino beams. Since the background for muon identification is generally much smaller than in the case of the electron, we use  $f = 0.01$  for both the neutrino factory and the conventional neutrino beam. A distinctive peak corresponding to the value of  $\Delta m_{32}^2 L$  where the oscillation is at a maximum can be found and the position of the peak is a good measurement of  $\Delta m_{32}^2$ . Here the figure of merit can be large for all energies with longer distances favoring measurements at higher energies. The total figure of merit as shown in Fig. 11.

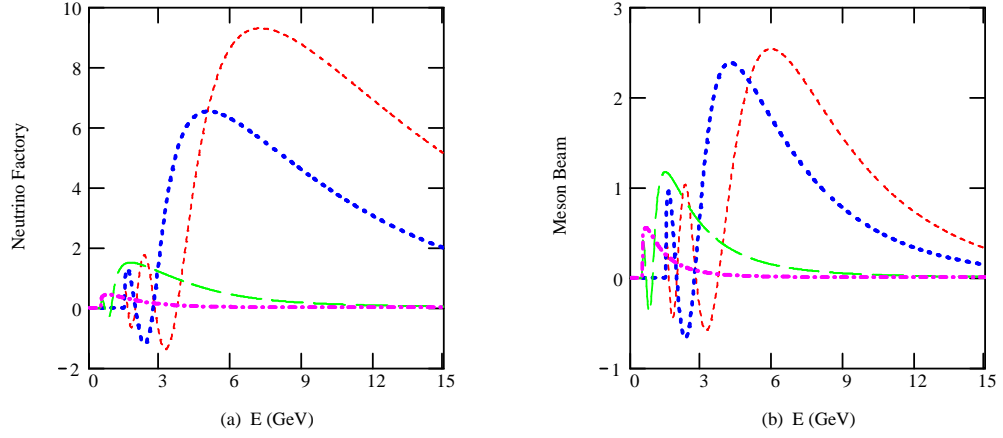


Figure 8: Figure of merit for the matter effect at a) neutrino factories with  $f=0.02$  and  $r=0.1$ , and b) meson-neutrino beams with  $f=0.03$  and  $r=0.1$ . The vertical axis is the figure of merit given by Eq. (24) and the horizontal axis is the neutrino energy.

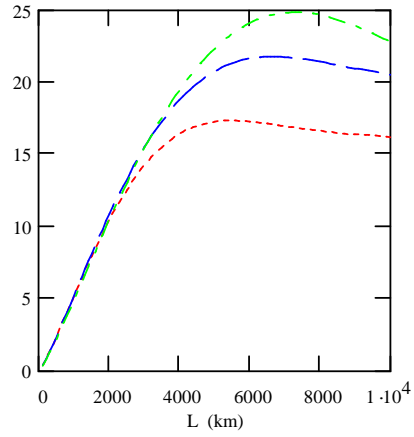


Figure 9: The total figure of merit of the matter effect for three neutrino factories: 20 GeV (dot), 30 GeV (dash), and 50 GeV (dashdot). The horizontal axis is the baseline length and the vertical axis is the total figure of merit.

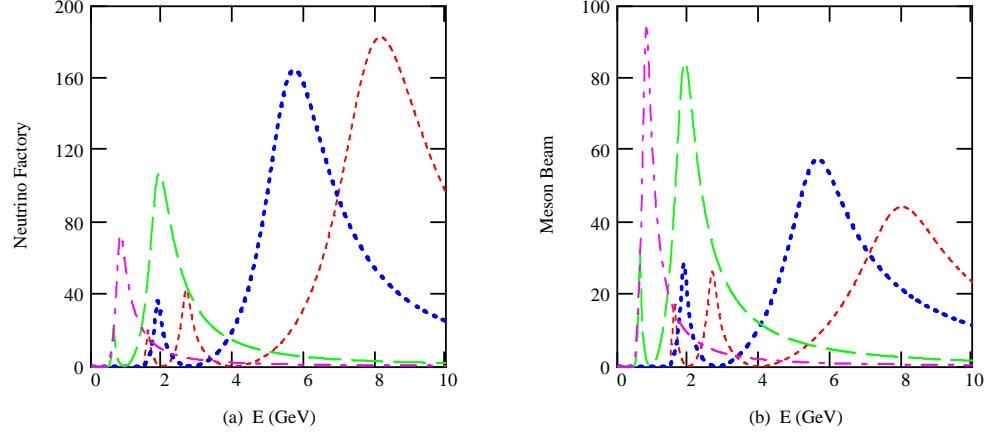


Figure 10: Figure of merit for  $\Delta m_{32}^2$  and  $\sin^2 2\theta_{23}$  at a) neutrino factories with  $f=0.01$  and  $r=0.1$ , and b) meson-neutrino beams with  $f=0.01$  and  $r=0.1$ . The vertical axis is the figure of merit given by Eq. (25) and the horizontal axis is the neutrino energy.

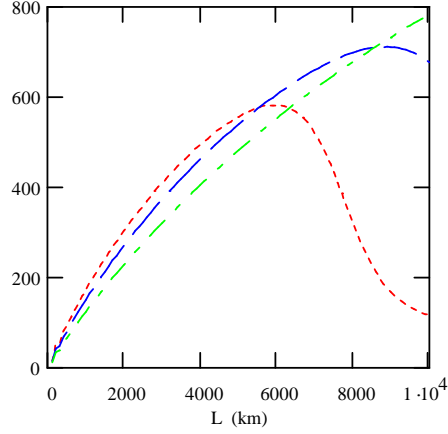


Figure 11: The total figure of merit for  $\Delta m_{32}^2$  and  $\sin^2 2\theta_{23}$  for the three neutrino factories: 20 GeV (dot), 30 GeV (dash), and 50 GeV (dashdot). The horizontal axis is the baseline length and the vertical axis is the total figure of merit.



#### 4.6 $\nu_\mu \rightarrow \nu_\tau$ Appearance

The appearance of  $\nu_\tau$  from a  $\nu_\mu$  beam is an unambiguous signal of the  $\nu_\mu \rightarrow \nu_\tau$  oscillation. Precision measurement of this oscillation probability is crucial in establishing the oscillation patterns and in determining whether or not  $\nu_\mu \rightarrow \nu_\tau$  is the only dominant oscillation mode or if there is still room for the  $\nu_\mu \rightarrow \nu_s$  oscillation, where  $\nu_s$  is a sterile neutrino. Although we expect that in the next few years, K2K and/or OPERA will observe the production of  $\tau$  because of the large  $\nu_\mu \rightarrow \nu_\tau$  probability, it is desirable that future detectors possess good  $\tau$  identification capability. The figure of merit can be written as

$$F_M^{(6)}(L) = \frac{\langle P_{\nu_\mu \rightarrow \nu_\tau}(L) \rangle}{\sqrt{\frac{\langle P_{\nu_\mu \rightarrow \nu_\tau}(L) \rangle + f}{N_{0\nu_\tau}(L)} + r^2 f^2 + (g \langle P_{\nu_\mu \rightarrow \nu_\tau}(L) \rangle)^2}} \quad (26)$$

Figure 12 shows this figure of merit as a function of energy at different baselines. It is expected that the error in the present case will be larger than measurements of other physical variables due to  $\tau$  event selection. Hence we set  $f=0.03$  for both neutrino factories and meson-neutrino beams. Due to the threshold of tau production, we made a cutoff at  $E_\nu = 4$  GeV. For the neutrino factory the larger distance is always better. For the meson beam 2100 km is also better than 300 km for neutrino energy above 6 GeV.

The total figure of merit is shown in Fig. 13. As shown, for  $L > 1000$  km the total figure of merit favors factory of higher energy. However, since the figure of merit of all factories are high, it is not necessary to maximize the figure of merit. A 20 GeV neutrino factory is more than adequate.

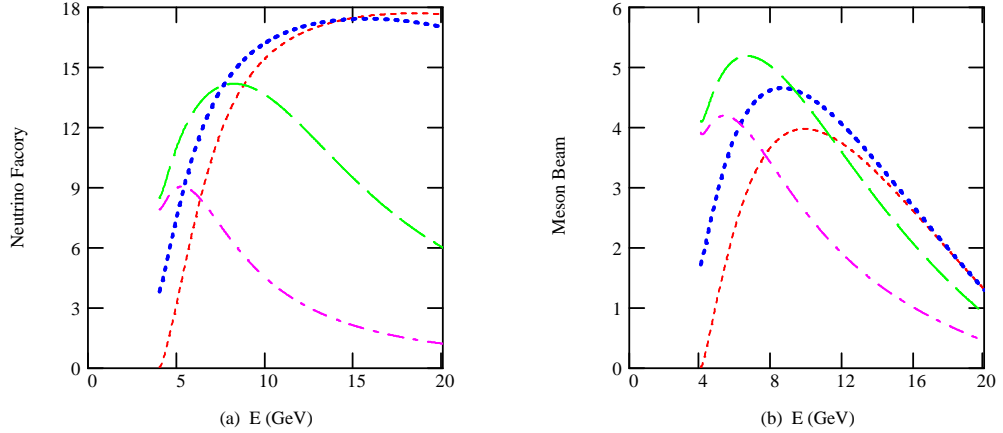


Figure 12: Figure of merit for tau appearance at a) neutrino factories with  $f=0.03$  and  $r=0.1$ , and b) meson-neutrino beams with  $f=0.03$  and  $r=0.1$ . The vertical axis is the figure of merit given by Eq. (26) and the horizontal axis is the neutrino energy.

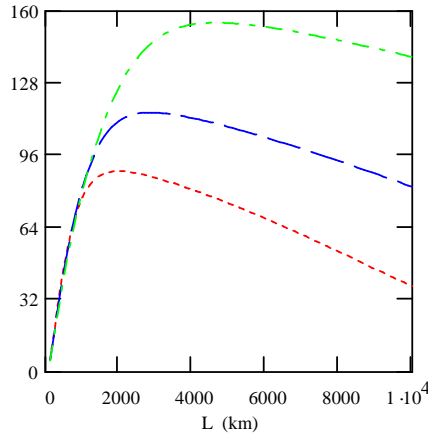


Figure 13: The total figure of merit for the  $\tau$  appearance measurement for the three neutrino factories: 20 GeV (dot), 30 GeV (dash), and 50 GeV (dashdot). The horizontal axis is the baseline length and the vertical axis is the total figure of merit.

## 5 Summary and Comments

In Table 2 we list the maximal values of all the figures of merit for all the measurements considered in the range 0.5 to 20 GeV for a neutrino factory of 20 GeV muon and a superbeam of 50 GeV primary proton. To put things in perspective, a few remarks are due. The value of the figure of merit is equal to the same value of  $\sigma$  in statistical significance. For a meaningful measurement we need to have a figure of merit no less than 3. Since the values of the figure of merit are obtained in this paper with explicit assumptions about the neutrino flux, the detector size, and the running time, we cannot take the values in the table too literally. However, as discussed in the preceding section, the relative merits of different baseline, which are not too sensitive to the explicit experimental conditions, are meaningful. The table shows that a longer baseline is preferred over a shorter one for the neutrino factory. For the meson neutrino beams, the preference depends on the variables measured but longer baseline length is generally slightly more preferred. For a more complete measurement of all the relevant variables, the combination of a relatively short and long baselines, such as 300 and 2100 km, will do a much better job.

The CP phase measurement is a challenging case. The values of the associated figure of merit at individual energies are generally small in all the cases we have considered. This will be true even for the total figure of merit in the case of superbeam. For the neutrino factory the value of the total figure of merit is already reasonably large at 2100 km for the 20 GeV factory. Generally speaking it is desirable to improve the statistics by improving the running conditions in all aspects: the beam luminosity, the running time, and the detector size.

Since the flux of the neutrino factory given in Eq. (5) is realistic, it is appropriate to make some detailed observation in the case of neutrino factory on the dependence of the figure of merit on the primary muon energy and baseline length:

(a) First consider the figure of merit at a fixed distance as a function of the neutrino energy. From the neutrino flux of the neutrino factory, Eq. (5), it can be seen that for a given neutrino energy and  $n_0^{(f)}$ , the neutrino flux decreases with increasing  $E_\mu$  for  $E_\mu > 4E_\nu/3$ . Therefore at a

|   | neutrino factory |         | meson-neutrino beam |         |
|---|------------------|---------|---------------------|---------|
|   | 300 km           | 2100 km | 300 km              | 2100 km |
| $\sin^2 2\theta_{13}$                       | 6.0              | 13      | 5.2                 | 3.9     |
| CP phase $\delta$                           | 0.55             | 1.1     | 0.6                 | 0.5     |
| sign of $\Delta m_{32}^2$                   | 0.7              | 8.0     | 1.0                 | 3.2     |
| matter effects                              | 0.5              | 6.6     | 0.6                 | 2.4     |
| $\Delta m_{32}^2$ and $\sin^2 2\theta_{23}$ | 75               | 165     | 95                  | 58      |
| $\tau$ appearance                           | 9                | 17.5    | 4.2                 | 4.7     |

Table 2: Summary of relative figures of merit (at the maxima) for various measurements at the baselines  $L=300$  and  $2100$  km.

given baseline, the maxima of the figures of merit of the various measurements moves to higher neutrino energies, in all cases very slowly, when  $E_\mu$  increases, while the height of the maximum generally decreases significantly. This is born out in our investigation of the 30 GeV and 50 GeV factories.

(b) Next consider the total figure of merit as a function of the baseline obtained by integrating the figure of merit over the whole available energy range at a fixed baseline. The total figure of merit increases almost linearly with baseline, starting at small baseline, with the values of the total figure of merit about the same for all three factories. The values of the figure of merit of the three factories will separate with further increases in the baseline. The lower energy factory will reach a maximum first. All the maxima are very broad. The first maximum in all the variables is reached by the 20 GeV factory at about 2000 km for the tau appearance experiment.

(c) All the values of the total figure of merit for the neutrino factories we considered are very significant, larger than 10, for baseline beyond 2000 km, except for the CP phase. The figure of merit for the CP phase of  $90^\circ$  has maxima in the 3500 km and 4000 km region. The height of the maximum decreases with increasing neutrino factory energy. The 20 GeV factory has the maximum figure of merit value of 4.5 at 3500 km and at 2000 km it is 3.6, which are reasonably large.

(d) Based on the above two considerations the lower energy factory of 20 GeV is preferable considering its lower budget of construction and possibly higher physics output. However for a more complete investigation, a detailed simulation on the actual number of events should be performed.

(e) All of the studies on neutrino factories use similar principles in determining the best  $L$  and  $E$  combination, i.e., there is some goodness of fit criterion. The differences are in the details, such as which sources of uncertainties are included, the particular values assigned, and whether or not error correlations are taken into account. Our total figure of merit for neutrino factories gives results similar to those obtained in other studies. For example, we find that the optimum  $L$  for detecting a nonzero  $\sin^2 2\theta_{13}$  in a neutrino factory is about 6000–7000 km, and that higher stored muon energies do better; similar conclusions are reached in Ref. [19, 20]. The optimum  $L$  for detection of  $CP$  violation is 3000–4000 km, which agrees with similar studies [16, 17, 18, 19, 20]. We find that the optimum  $L$  for determining the sign of  $\Delta m_{32}^2$  is around 5000 km, consistent with the conclusions of Refs. [17] and [20]. However, we have also systematically applied the figure of merit to other oscillation variables, such as the matter effect,  $\nu_\tau$  appearance and  $\theta_{23}$ , most of which have not been applied before. Furthermore, we have made a comparison of neutrino factories and meson neutrino beams using identical criteria.

Although we have not considered the total figure of merit for the case of the meson neutrino

due to the lack of generally valid beam energy profile, we can nevertheless draw some useful conclusions based on the salient features of the differential figure of merit. The maximum of the figure of merit at a shorter baseline tend to be sharply peaked, while that of a longer baseline is broad. Hence the total figure of merit integrated around the maximum will favor longer baselines. Naively integrating the differential figure of merit over the envelope of the beam intensity, Eq. (6), shows that the values at 2100 km are larger than at 300 km.

Finally, we note that in the present work, we focus on the statistical significance of long and very long baselines in the energy range of 0.5-20 GeV. Consequently the dominant mass scale is the atmospheric neutrino scale, i.e.,  $\Delta m_{32}^2$ . For neutrino energies of a few hundred MeV or smaller, the effect of the solar neutrino scale becomes important. Therefore a separate investigation is necessary.

## Acknowledgement

We would like to thank Dr. Xinmin Zhang and Dr. Lianyou Shan for helpful assistance. We would also like to thank our colleagues of the H2B collaboration [8] for support. This work is supported in part by DOE Grant No. DE-FG02-G4ER40817.

## References

- [1] Y. Fukuda *et al.*, Phys. Rev. Lett. **B 81** (1998) 1562.
- [2] Some recent reviews on the experimental status of neutrino oscillation can be found in:  
J.M. Conrad, *Recent Results on Neutrino Oscillations*, arXiv: hep-ex/9811009  
L. Di Lella, *Accelerator and Reactor Neutrino Experiments*, arXiv: hep-ph/9912010  
W.A. Man, *Atmospheric Neutrino and the Oscillation Bonanza*, arXiv: hep-ex/9912007  
Talks at recent neutrino Conferences, e.g., "NOW 2000" and "Neutrino 2000" be found on the "Neutrino Industry" website: <http://www.hep.anl.gov/ndk/hypertext/nuindustry.html>
- [3] J2K: Y. Ito, et. al., *Letter of Intent: A Long Baseline Neutrino Oscillation Experiment the JHF 50 GeV Proton-Synchrotron and the Super-Kamiokande Detector*, JHF Neutrino Working Group, Feb. 3, 2000. The JHF is renamed as HIPA.
- [4] HIPA: A multipurpose high intensity proton synchrotron at both 50 GeV and 3 GeV to be constructed at the Jaeri Tokai Campus, Japan has been approved in December, 2000 by the Japanese funding agency. The long baseline neutrino oscillation experiment is one of the projects of the particle physics program of the facility. More about HIPA can be found at the website: <http://jkj.tokai.jaeri.go.jp>
- [5] MINOS: P. Adamson, et al., *The MINOS Detector Technical Design Report*, October 1998, Fermilab Report NuMI-L-337.
- [6] ICARUS: J.P. Revol, et al., *A Search Program for Explicit Neutrino Oscillations at Long and Medium Baseline with ICARUS Detectors*, ICARUS-TM-97/01, 5 March 1997; A. Bettini, et al., Nucl. Instr. Methods, **A332**, 395 (1993).
- [7] OPERA: *A Long Baseline  $\nu_\tau$  Appearance Experiment in CNGS from CERN to Gran Sasso*, Progress Report, CERN/SPSC, LNBS-LOI 19/99, August 27, 1999.
- [8] H2B: Hesheng Chen, et al., *Study Report: H2B, Prospect of a very Long Baseline Neutrino Oscillation Experiment, HIPA to Beijing*, March 19, 2001, VLBL Study Group-H2B-1; IHEP-EP-2001-01; AS-ITP-01-004; Ames-HET 01-01; arXiv: hep-ph/0104266.
- [9] M. Aoki, K. Hagiwara, U. Hayato, T. Kobayashi T. Nakaya, K. Nishikawa and N. Okamura, to be published in the Proceeding of BCP4, Ise, Japan, Feb. 19-23, 2001; arXiv: hep-ph/0104220.
- [10] C. Albright, et al., *Physics at a neutrino factory*, arXiv:hep-ph/0008064.
- [11] S. Geer, Phys. Rev. **D57**, 6989 (1999).
- [12] V. Barger, S. Geer, K. Whisnant, Phys. Rev. **D61**, 053004 (2000) (arXiv:hep-ph/9906487).
- [13] A. Malensek, Fermilab note FN-341, 1981; J.E. McDonald and D. Naples, MINOS Note NuMI-B-570, 1999.
- [14] M. Bonesini, A. Marchionni, F. Pietropaolo, and T. Tabarelli de Fatis, Eur. Phys. J., **C20**, 13 (2000) (arXiv:hep-ph/0101163).
- [15] The numerical cross sections up to the lab energy of 100 GeV are obtained from the MINOS Collaboration, D. Casper, private communication.
- [16] A. Donini, M.B. Gavela, P. Hernández and S. Rigolin, Nucl. Phys. **B574**, 23 (2000) (arXiv: hep-ph/9909254); A. Cervera *et al.*, Nucl. Phys. **B579**, 17 (2000) (arXiv: hep-ph/0002108); A. Bueno, M. Campanelli and A. Rubbia, Nucl. Phys. **B589**, 577 (2000) (arXiv: hep-ph/0005007).
- [17] V. Barger, S. Geer, R. Raja, and K. Whisnant, Phys. Rev. **D62**, 073002 (2000) (arXiv: hep-ph/0003184); Phys. Rev. **D63**, 113011 (2001) (arXiv: hep-ph/0012017).

- [18] J. Burguet-Castell, M.B. Gavela, J.J. Gomez Cadenas, P. Hernandez, and O. Mena, Nucl. Phys. **B608**, 301 (2001) (arXiv: hep-ph/0103258).
- [19] M. Freund, P. Huber, and M. Lindner, Nucl. Phys. **B615**, 331 (2001) (arXiv: hep-ph/0105071).
- [20] J. Pinney and O. Yasuda, Phys. Rev. **D64**, 093008 (2001) (arXiv: hep-ph/0105087).
- [21] M.C. Gonzalez-Garcia, M. Maltoni, C. Peña-Garay and J.W.F. Valle, Phys. Rev. **D63**, 033005 (2001) (arXiv: hep-ph/0009350).
- [22] Treatments of quasi-elastic interactions, in particular including the threshold effect of the  $\tau$  production, can be found in L.J. Hall and H. Murayama, Phys. Lett. **B 463**, 241 (1999) (arXiv: hep-ph/9810468); E.A. Paschos and J.Y. Yu, *Neutrino Interactions in Oscillation Experiments*, DO-TH 01/08, arXiv: 0107261.
- [23] For the discussion of a 100 kt water Čerenkov calorimetric detector see, Ref. [8] and Y.F. Wang, talk given at “New Initiatives in Lepton Flavor Violation and Neutrino Oscillations with Very Intense Muon and Neutrino Sources”, Oct. 2-6, 2000, Hawaii, U.S.A.; arXiv: hep-ex/0010081
- [24] V. Barger, S. Geer, R. Raja, and K. Whisnant, Phys. Rev. **D62**, 013004 (2000) (arXiv: hep-ph/9911524).
- [25] Zhi-zhong Xing, Phys. Lett. **B487**, 327 (2000) (arXiv: hep-ph/0002246).
- [26] M. Freund, H. Huber, and M. Linder, Nucl. Phys. **B585** 105 (2000) (arXiv: hep-ph/0004085)